Pergamon

Int. J. Solids Structures Vol. 34, Nos 33–34, pp. 4305–4326, 1997

0020–7683/97 $17.00 + .00

PII: S0020–7683(97)00025–5

EFFECT OF INTERFACIAL COMPLIANCE ON BIFURCATION OF A LAYER BONDED TO A SUBSTRATE

D. BIGONI
Istituto di Scienza delle Costruzioni—Facoltà di Ingegneria, Università di Bologna, 40136 Bologna, Italy

M. ORTIZ
Division of Engineering and Applied Science, California Institute of Technology, Pasadena, CA 91125, U.S.A.

and

A. NEEDLEMAN
Division of Engineering, Brown University, Providence, RI 02912, U.S.A.

(*Received* 19 *June* 1996; *in revised form* 27 *December* 1996)

Abstract—The effect of interfacial compliance on the bifurcation of a layer bonded to a substrate is analyzed. The bifurcation problem is formulated for hyperelastic, layered solids in plane strain. Attention is then confined to the problem of a layer of finite thickness on a half-space. The layer and substrate are subject to plane strain compression, with the compression axis parallel to the bond line. The materials in the layer and in the half-space are taken to be incrementally linear, incompressible solids, with most results presented for Mooney–Rivlin and J_2-deformation theory constitutive relations. The limiting case of an undeforming half-space is also considered. The interface between the layer and the substrate is characterized by an incrementally linear traction rate vs velocity jump relation, so that a characteristic length is introduced. A variety of bifurcation modes are possible depending on the layer thickness, on the constitutive parameters of the layer and the substrate, and on the interface compliance. These include shear band modes for the layer and the substrate, and diffuse instability modes involving deformation in the layer and the substrate. For a sufficiently compliant interface, the mode with the lowest critical stress is a long (relative to the layer thickness) wavelength plate-like bending mode for the layer. © 1997 Elsevier Science Ltd.

1. INTRODUCTION

The stability of layered structures is a concern in a broad range of contexts including sandwich panels in aircraft, submarine coatings, integrated circuits and the origin of geological formations. There is accordingly a large amount of literature where stability of layered media is investigated from a variety of perspectives; see, for example, Biot (1965), Dorris and Nemat-Nasser (1980), Steif (1986a, b; 1987; 1990), Papamichos *et al.* (1990), Dowaikh and Ogden (1991), Benallal *et al.* (1993), Triantafyllidis and Lehner (1993), Triantafyllidis and Leroy (1994), Shield *et al.* (1994), Ogden and Sotiropoulos (1995) and Steigmann and Ogden (1996) and references cited therein. The loss of stability can lead to the loss of cohesion between layers. In previous investigations, perfect bonding has been assumed between the layers. Here, the effect of a finite, non-zero interfacial compliance on the stability of layered structures is analyzed and the results show that reduced cohesion between layers can promote instability.

The general problem of the finite deformation of a layered, hyperelastic, incompressible material in plane strain is formulated. The interfaces between layers are modeled by a constitutive relation expressed in terms of a linear relation between the velocity jump across the interface and the nominal traction rate across the interface, so that dimensional considerations introduce an interface characteristic length. Attention is focused on the specific problem of a layer of finite thickness bonded to a half-space and subject to plane

strain compression, with the compression axis parallel to the bond line. The fundamental path is taken to correspond to equal deformations in the layer and the half-space. Bifurcation from this state is considered. There are two characteristic lengths; that associated with the interface description and the layer thickness.

Results are presented for two constitutive models, a Mooney–Rivlin material and a J_2-deformation theory material. The results for both material models illustrate the role that interfacial compliance can play in reducing the stress level at which bifurcation occurs. In previous work, Suo *et al.* (1992) have carried out a general investigation of the effect of interfacial compliance on the stability of two semi-infinite solids bonded along a planar interface, Keer *et al.* (1982) have investigated a homogeneous half-space with an array of cracks parallel to the free surface and found a substantial reduction in the bifurcation load because of the presence of the cracks, and Steif (1990) has analyzed the bifurcation of two plane strain infinite media in contact and noted that tangential slip between the two media gave a reduction in the bifurcation strain. Here, for the case of a thin layer on a stiff substrate it is found that interfacial compliance gives a pronounced reduction in the bifurcation stress and changes the bifurcation mode. With a compliant interface, the bifurcation mode becomes a plate-like bending mode for the layer, which leaves the substrate almost undeformed, as opposed to a stationary-wave mode, which involves both media. Moreover, for the J_2-deformation theory constitutive relation, a variety of bifurcation modes are found, including plate-like buckling for the layer and stationary waves-like modes involving both the layer and the substrate, as well as interfacial, surface and shear band modes in either the layer or the substrate. The occurrence of one or another of these modes is related to the material and interface parameters, as well as to the layer thickness and the boundary conditions. This variety of bifurcation modes is consistent with the experimental observation on Cu–W laminates by Özturk *et al.* (1991), where, when failure is approached, a "competition" between shear banding and diffuse bifurcation modes was observed.

2. PROBLEM FORMULATION

A laminated structure, as shown in Fig. 1, is considered. In the prebifurcation state, all layers are specified to undergo the same homogeneous deformation so that equilibrium and compatibility are trivially satisfied. Furthermore, plane strain conditions are assumed to prevail, with the principal directions of deformation aligned normal and parallel to the layers. Rate boundary conditions consistent with continuing deformation in the homogeneous mode are prescribed and the possibility of bifurcation from the homogeneous state is investigated.

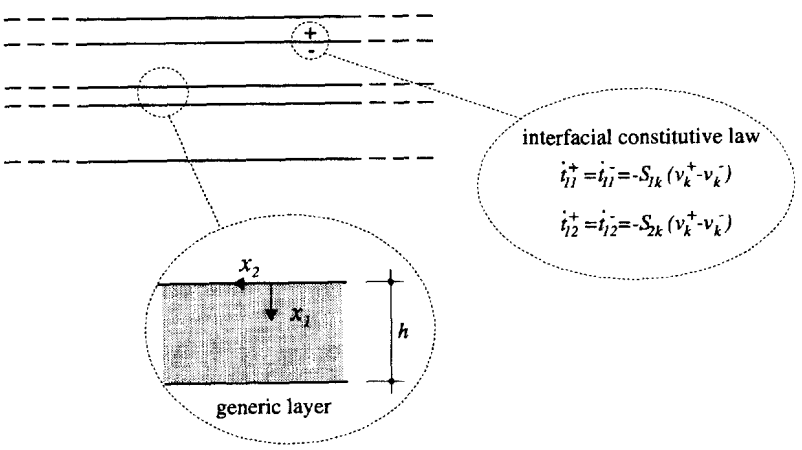

Fig. 1. Sketch of the laminated structure analyzed. The layers can have different thickness and correspond to different elastic materials. The interfaces between the layers have a specified interfacial compliance. The nominal tractions are required to vanish on any external surface.

A Lagrangian formulation of the field equations is used with the current state taken as reference. Material points are identified by their Cartesian coordinates in the reference state. Suppose that at some stage of the deformation history, two solutions are possible to the rate equilibrium equations. Denote the difference between rate field quantities associated with two possible solutions by $(\dot{})$. In terms of the unsymmetric nominal stress tensor, $\mathbf{t}$, which is related to the traction transmitted across a material element of area having normal $\mathbf{n}$ in the reference configuration by $\mathbf{T} = \mathbf{n} \cdot \mathbf{t}$, the difference fields must satisfy

$$\dot{t}_{ij,i} = 0, \tag{1}$$

where Cartesian tensor notation is used with a comma denoting partial differentiation and, for plane strain, indices range from 1 to 2.

The materials considered are rate independent and incompressible, with the rate constitutive relation having the form

$$\dot{t}_{ij} = K_{ijkl} v_{l,k} + \dot{p}\delta_{ij}. \tag{2}$$

Here, δ_{ij} is the Kronecker delta, $\dot{p}$ is the hydrostatic stress rate (positive in tension) and K_{ijkl} are the instantaneous moduli, which are presumed to possess the symmetries $K_{ijkl} = K_{klij}$.

In addition to (2), incompressibility requires

$$v_{i,i} = 0, \tag{3}$$

where $\mathbf{v}$ denotes the velocity.

With the coordinate system in Fig. 1, attention is restricted to layered solids that are unbounded in the x_2 direction. Any external surface has its normal parallel to the x_1 direction and is taken to be subject to dead loading so that for the bifurcation problem

$$\dot{t}_{11} = 0, \quad \dot{t}_{12} = 0. \tag{4}$$

At each interface between layers, the boundary conditions are that the traction rate is continuous across the interface and that this traction rate is related to the velocity jump across the interface by an elastic interfacial constitutive relation. These require that

$$\dot{t}^{+}_{11} = \dot{t}^{-}_{11} = \dot{t}_{11} \quad \dot{t}^{+}_{12} = \dot{t}^{-}_{12} = \dot{t}_{12}, \tag{5}$$

and

$$\dot{t}_{11} = -S_{1k}(v^{+}_{k} - v^{-}_{k}), \quad \dot{t}_{12} = -S_{2k}(v^{+}_{k} - v^{-}_{k}), \tag{6}$$

with the superscripts $+$ and $-$ referring to quantities on opposite sides of the interface as sketched in Fig. 1. The sign convention in (6) is such that the x_1-axis is directed towards $(-)$ and away from $(+)$.

In plane strain, the instantaneous stiffness of the interface, $\mathbf{S}$, is a 2×2 matrix of dimension [stress/length], which may depend on the deformation jump history up to the current state, but is independent of the current velocity jump. Whatever the history dependence, the key feature of the interface response is that, with increasing separation, the traction across the interface reaches a maximum and then decreases. For a softening interface, one or more eigenvalues of $\mathbf{S}$ are negative. The limiting cases of a traction free surface and a perfectly bonded interface correspond to $\mathbf{S} \equiv 0$ and $\mathbf{S} \to \infty$, respectively.

In each layer, bifurcations of the form

$$v_l = w_l(x_1)e^{ikx_2}, \quad \dot{p} = q(x_1)e^{ikx_2}, \tag{7}$$

are sought. The functions $w_l(x_1)$ and $q(x_1)$ will, in general, differ from layer to layer but the wave number k is taken to be the same for all layers.

Substituting (7) with (2) into (1) gives

$$\begin{aligned} &K_{1111}w_1'' + K_{1112}w_2'' + ik(K_{1121}+K_{2111})w_1' + ik(K_{1122}+K_{2112})w_2' \\ &\quad -k^2K_{2121}w_1 - k^2K_{2122}w_2 + q' = 0, \\ &K_{1211}w_1'' + K_{1212}w_2'' + ik(K_{1221}+K_{2211})w_1' + ik(K_{1222}+K_{2212})w_2' \\ &\quad -k^2K_{2221}w_1 - k^2K_{2222}w_2 + ikq = 0, \end{aligned} \tag{8}$$

where $(\,)'$ denotes differentiation with respect to x_1.

Equations (8) and the incompressibility condition

$$w_1' + ikw_2 = 0, \tag{9}$$

constitute three constant coefficient ordinary differential equations for the three unknown functions $w_1(x_1)$, $w_2(x_1)$ and $q(x_1)$.

2.1. *Material behavior*

For orthotropic, incompressible, rate independent solids deforming in plane strain, Biot (1965) has shown that the incremental response is governed by two in-plane shearing moduli. With μ and μ_* denoting the moduli corresponding to shearing parallel to the principal stress axis and shearing at 45°, the components of the instantaneous moduli **K** in (2) have the form (Biot, 1965; Hill and Hutchinson, 1975)

$$\begin{aligned} &K_{1111} = \mu_* - \frac{\sigma}{2} - p, \quad K_{1122} = -\mu_*, \quad K_{1112} = K_{1121} = 0, \\ &K_{2211} = -\mu_*, \quad K_{2222} = \mu_* + \frac{\sigma}{2} - p, \quad K_{2212} = K_{2221} = 0, \\ &K_{1212} = \mu + \frac{\sigma}{2}, \quad K_{1221} = \mu - p, \quad K_{2121} = \mu - \frac{\sigma}{2}, \end{aligned} \tag{10}$$

with

$$\sigma = \sigma_1 - \sigma_2, \quad p = \frac{\sigma_1 + \sigma_2}{2}. \tag{11}$$

Subsequently, numerical examples are given for two specific materials, both of which are initially isotropic elastic solids. One is the Mooney–Rivlin material for which the strain energy, W, in plane strain is given by

$$W = \frac{\mu_0}{2}(\lambda_1^2 + \lambda_2^2 - 2), \tag{12}$$

where λ_1 and λ_2 are the principal in-plane stretches. In the current state, $\lambda_1 = \lambda$ and $\lambda_2 = 1/\lambda$. For the Mooney–Rivlin material

$$\sigma = \mu_0(\lambda^2 - \lambda^{-2}), \quad \mu_* = \mu = \frac{\mu_0}{2}(\lambda^2 + \lambda^{-2}). \tag{13}$$

The other material is a J_2-deformation theory solid introduced by Hutchinson and

Neale (1979). For power law hardening in plane strain, the strain energy function is given by

$$W = \frac{\sigma_0 \varepsilon_0}{1+N}\left(\frac{\varepsilon_e}{\varepsilon_0}\right)^{1+N}, \quad \varepsilon_e = \sqrt{\frac{2}{3}[(\ln \lambda_1)^2 + (\ln \lambda_2)^2]}. \tag{14}$$

Here, σ_0 and ε_0 are material constants (for the pure power law hardening in (14) these enter only in the combination σ_0/ε_0^N) and μ, μ_* and σ are given by

$$\sigma_e = \sigma_0 \left(\frac{\varepsilon_e}{\varepsilon_0}\right)^N, \tag{15}$$

$$\mu_* = \frac{N\sigma_0}{3\varepsilon_0}\left(\frac{\varepsilon_e}{\varepsilon_0}\right)^{N-1}, \quad \mu = \frac{\sigma_0}{\sqrt{3}}\left(\frac{\varepsilon_e}{\varepsilon_0}\right)^N \coth(\sqrt{3}\varepsilon_e), \tag{16}$$

with $\varepsilon_e = 2\varepsilon/\sqrt{3}$, $\varepsilon = \ln \lambda$ and $\sigma_e = \sqrt{3}\sigma/2$.

The significance of the J_2-deformation theory solid is that it can serve as Hill's (1958) linear comparison solid for an elastic–plastic solid with a corner on its yield surface, see, for example, Christoffersen and Hutchinson (1979). Briefly, for elastic–plastic solids exhibiting piecewise linear behavior, the neighborhood of the current state in strain rate space can be divided into a number of cones, in each of which a linear relationship between stress rate and strain rate holds. For example, the constitutive relation for the classical elastic–plastic solid is piecewise linear with two branches; one for plastic loading and the other for elastic unloading. Hill (1958) has shown that for elastic–plastic solids and for a pre-bifurcation state corresponding to continued plastic loading, the first possible bifurcation can be investigated for a solid having moduli that are independent of rate quantities and that correspond to the active moduli in the pre-bifurcation state. The solid with these moduli is termed the linear comparison solid.

2.2. *General solution*

The solution to the system of homogeneous ordinary differential eqns (8) and (9) has the form

$$w_l(x_1) = a_l e^{\tau x_1}, \quad q(x_1) = c e^{\tau x_1}.$$

Substituting into (8) and (9) and using (10) gives

$$\begin{bmatrix} \left(\mu_* - \frac{\sigma}{2} - p\right)\tau^2 - k^2\left(\mu - \frac{\sigma}{2}\right) & i\tau k(\mu - \mu_* - p) & \tau \\ i\tau k(\mu - \mu_* - p) & \tau^2\left(\mu + \frac{\sigma}{2}\right) - \left(\mu_* + \frac{\sigma}{2} - p\right)k^2 & ik \\ \tau & ik & 0 \end{bmatrix} \begin{bmatrix} a_1 \\ a_2 \\ c \end{bmatrix} = \begin{bmatrix} 0 \\ 0 \\ 0 \end{bmatrix}. \tag{17}$$

Setting the determinant of coefficients in (17) to zero determines the four values of the exponent τ as

$$\tau_{1,2} = \pm k\sqrt{\frac{2\mu-4\mu_*+\Lambda}{-2\mu-\sigma}}, \tag{18}$$

$$\tau_{3,4} = \pm k\sqrt{\frac{2\mu-4\mu_*-\Lambda}{-2\mu-\sigma}}, \tag{19}$$

where

$$\Lambda = \sqrt{\sigma^2-16\mu_*(\mu-\mu_*)}. \tag{20}$$

Therefore, assuming that the roots are distinct, the general solution for $w_1(x_1)$, $w_2(x_1)$ and $q(x_1)$ has the form

$$w_l(x_1) = \sum_{j=1}^{4} b_j a_l^j e^{\tau_j x_1}, \quad q(x_1) = \sum_{j=1}^{4} b_j c^j e^{\tau_j x_1}, \tag{21}$$

where b_j are arbitrary coefficients and (a_l^j, c^j) is the eigenvector of (17) corresponding to eigenvalue τ_j.

The solutions are

$$w_1(x_1) = b_1 e^{\tau_1 x_1} + b_2 e^{-\tau_1 x_1} + b_3 e^{\tau_3 x_1} + b_4 e^{-\tau_3 x_1}, \tag{22}$$

$$w_2(x_1) = i\left[\frac{\tau_1}{k}(b_1 e^{\tau_1 x_1} - b_2 e^{-\tau_1 x_1}) + \frac{\tau_3}{k}(b_3 e^{\tau_3 x_1} - b_4 e^{-\tau_3 x_1})\right], \tag{23}$$

$$q(x_1) = \frac{\tau_1(\sigma+\Lambda)}{2}(b_1 e^{\tau_1 x_1} - b_2 e^{-\tau_1 x_1}) + \frac{\tau_3(\sigma-\Lambda)}{2}(b_3 e^{\tau_3 x_1} - b_4 e^{-\tau_3 x_1}). \tag{24}$$

Using (2), (10) and (7) in (5), continuity of tractions across an interface takes the form

$$\left(2\mu_*^+ - \frac{\sigma^+}{2} - p^+\right)(w_1^+)' + q^+ = \left(2\mu_*^- - \frac{\sigma^-}{2} - p^-\right)(w_1^-)' + q^-,$$

$$ik(\mu^+ - p^+)w_1^+ + \left(\mu^+ + \frac{\sigma^+}{2}\right)(w_2^+)' = ik(\mu^- - p^-)w_1^- + \left(\mu^- + \frac{\sigma^-}{2}\right)(w_2^-)', \tag{25}$$

and the interfacial constitutive relation (6) becomes

$$\left(2\mu_* - \frac{\sigma}{2} - p\right)w_1' + q = -S_{11}(w_1^+ - w_1^-) - S_{12}(w_2^+ - w_2^-), \tag{26}$$

$$ik(\mu - p)w_1 + \left(\mu + \frac{\sigma}{2}\right)w_2' = -S_{21}(w_1^+ - w_1^-) - S_{22}(w_2^+ - w_2^-), \tag{27}$$

where, from (25), the quantities on the left hand side of (27) can be associated with either the + or − side of the interface. Together, (25)–(27) constitute four equations for the eight unknown coefficients b_j^+ and b_j^-. The remaining equations come from the boundary conditions at the other edges of the + and − layers. For example, if the opposite edge of the + layer is traction free, the boundary condition there is of the form of (25) with the left hand sides set equal to zero; if the − layer is half-space that is unbounded for $x_1 \to \infty$, then the two coefficients of the terms with positive real exponents vanish. In any case, imposition of the boundary conditions gives a set of homogeneous equations for the

unknown constants in the layers. Setting the determinant of this set of equations to zero gives the critical condition for bifurcation.

The character of the exponents τ_i depends on the character of the governing equations. Using the standard classification of regimes, Hill and Hutchinson (1975), the τ_i are: (i) all real in the elliptic imaginary regime, (ii) two complex conjugate pairs in the elliptic complex regime, (iii) all pure imaginary in the hyperbolic regime, and (iv) two pure imaginary and two real in the parabolic regime. The significance of this is that a loss of ellipticity is associated with a shear band bifurcation. For the constitutive relations considered here, the rate equations are either elliptic or hyperbolic and the undeformed state is in the elliptic regime. For the Mooney–Rivlin material, the rate equations remain elliptic regardless of the magnitude of the deformations. On the other hand, for the J_2-deformation theory solid, the governing equations become hyperbolic when (Hutchinson and Tvergaard, 1981)

$$\varepsilon_e = \frac{2}{\sqrt{3}}\sqrt{N(r-N)}, \quad r = \sqrt{3}\varepsilon_e \coth(\sqrt{3}\varepsilon_e). \tag{28}$$

Thus, if the critical strain in (28) is reached in a layer before bifurcation into the layered solid mode (7), a shear band localization in that layer precedes the layered solid bifurcation.

3. RESULTS

3.1. *Layer on a half-space*

For a layer laying between $0 \leqslant x_1 \leqslant h$ on the half-space $x_1 \geqslant h$, the boundary conditions (4) apply at $x_1 = 0$ and the interface conditions (6) are imposed at $x_1 = h$. Additionally, the condition that the solution decays with depth in the half-space has to be imposed. The + field quantities are taken to be associated with the layer and the − field quantities with the half-space. Attention is focused on circumstances where bifurcation occurs while the material in both the layer and in the half-space is in the elliptic regime. With the signs in (18) and (19) chosen so that $\Re(\tau_1)$ and $\Re(\tau_3)$ are positive, b_1^- and b_3^- must vanish (note that in the hyperbolic regime the τ_i are all pure imaginary so that this condition cannot be imposed). The bifurcation condition becomes

$$\det(\mathbf{M}) = 0, \tag{29}$$

where $\mathbf{M}$ is the 6×6 coefficient matrix of the system of equations

$$\begin{bmatrix} M_{11} & M_{12} & M_{13} & M_{14} & M_{15} & M_{16} \\ M_{21} & M_{22} & M_{23} & M_{24} & M_{25} & M_{26} \\ M_{31} & M_{32} & M_{33} & M_{34} & M_{35} & M_{36} \\ M_{41} & M_{42} & M_{43} & M_{44} & M_{45} & M_{46} \\ M_{51} & M_{52} & M_{53} & M_{54} & M_{55} & M_{56} \\ M_{61} & M_{62} & M_{63} & M_{64} & M_{65} & M_{66} \end{bmatrix} \begin{bmatrix} b_1^+ \\ b_2^+ \\ b_3^+ \\ b_4^+ \\ b_2^- \\ b_4^- \end{bmatrix} = \begin{bmatrix} 0 \\ 0 \\ 0 \\ 0 \\ 0 \\ 0 \end{bmatrix}. \tag{30}$$

The expressions for the components of $\mathbf{M}$ are given in the Appendix assuming that $S_{12} = S_{21} = 0$. Thus, the results presented here are confined to the special case where the coupling between the normal and shear response is absent.

The bifurcation condition (29) involves the dimensionless parameters kh, $\mu_*^+/(hS_{11})$ and $\mu_*^+/(hS_{22})$. The wavenumber k can be written as $k = 2\pi/l$ where l is the wavelength of the bifurcation mode. With the coordinate system in Fig. 1, S_{11} corresponds to the normal stiffness of the interface and S_{22} to the shear stiffness of the interface. These moduli can be written as

$$S_{11} = \frac{C_n}{\delta_n}, \quad S_{22} = \frac{C_t}{\delta_t}, \tag{31}$$

where C_n and C_t have the dimension of stress, and δ_n and δ_t are normal and tangential interface characteristic lengths. The ratios $\mu_*^+/(hS_{11})$ and $\mu_*^+/(hS_{22})$ can then be written as

$$\frac{\mu_*^+}{hS_{11}} = \left(\frac{\delta_n}{h}\right)\left(\frac{\mu_*^+}{C_n}\right), \quad \frac{\mu_*^+}{hS_{22}} = \left(\frac{\delta_t}{h}\right)\left(\frac{\mu_*^+}{C_t}\right). \tag{32}$$

In general, the interface characteristic lengths δ_n and δ_t are expected to be small compared to the layer thickness h. The value of the interfacial stiffness will depend on the bonding of the layer and the substrate and, in general, will decrease with increasing interfacial separation; when the normal and tangential tractions across the interface reach a maximum the corresponding stiffness, C_n and C_t, respectively, vanishes. Hence, the values of μ_*^+/C_n and μ_*^+/C_t can be large.

In the numerical results presented subsequently, further simplifications are made. In most cases it is assumed that $C_n/\delta_n = C_t/\delta_t$. In a few calculations, C_t is taken to be zero (no interface shear stiffness). Hence, the bifurcation results depend on the ratio of layer thickness to bifurcation mode wavelength h/l and on the ratio of an interface characteristic length to layer thickness c/h, where

$$c = \delta_n\left(\frac{\mu_*^+}{C_n}\right). \tag{33}$$

The ratio c/h is zero for a perfectly bonded interface and the value of this ratio increases with increasing interface compliance. In the limit of zero interface stiffness, $c/h \to \infty$ and the interface becomes a free surface.

The prebifurcation state is taken to be specified by the principal extensions $\lambda_2 = 1/\lambda$, $\lambda_1 = \lambda$ on both sides of the interface (the 2-axis is parallel to the interface, as sketched in Fig. 1). For a perfectly bonded interface, continuity of the normal displacement gradient across the interface, together with incompressibility, requires the strain state to be the same on both sides of the interface. With a compliant interface, there can be a displacement jump across the interface, so that a difference in deformation state is possible. Here, it is presumed that the loading is such as to enforce the same strain state on both sides of the interface in the pre-bifurcation state. Results for Mooney–Rivlin and J_2-deformation theory materials are presented when the pre-bifurcation state corresponds to plane compression on each side of the interface, i.e., $\lambda \geqslant 1$, $\sigma_1^+ = \sigma_1^- = 0$ and $\sigma_2 < 0$.

3.1.1. *Mooney–Rivlin material.* It is assumed that both the layer and the substrate are Mooney–Rivlin materials homogeneous and unstressed in the ground state. Quantities with a + are associated with the layer and quantities with a − are associated with the substrate. From (13), with μ^+ and μ^- denoting the current incremental moduli for the layer and the substrate, respectively, the non-vanishing in-plane stress component is given by

$$\sigma_2^+ = -2\mu^+\left(\frac{\lambda^2-\lambda^{-2}}{\lambda^2+\lambda^{-2}}\right), \quad \sigma_2^- = -2\mu^-\left(\frac{\lambda^2-\lambda^{-2}}{\lambda^2+\lambda^{-2}}\right). \tag{34}$$

From (34) and (13) the following relation holds on the fundamental path,

$$\frac{\sigma_2^+}{\sigma_2^-} = \frac{\mu^+}{\mu^-} = \frac{\mu_0^+}{\mu_0^-} = \text{const.} \tag{35}$$

Using (35) in (18) to (20) the expressions for the exponents τ simplify to

$$\tau_1^+ = \tau_1^- = k\sqrt{\frac{2-|\sigma_2|/\mu}{2+|\sigma_2|/\mu}}, \quad \tau_3^+ = \tau_3^- = k. \tag{36}$$

Using (36), the components of the matrix **M** in (30) can be written in a simple form and the bifurcation stress is obtained from (29).

The results are presented in Figs 2–4 as plots of σ_2/μ vs h/l. From (34), $\sigma_2^+/\mu^+ = \sigma_2^-/\mu^-$ and the common value of this ratio is denoted by σ_2/μ. The ratio h/l is the ratio of the layer thickness divided by the wave length of the bifurcation mode, i.e., $l = 2\pi/k$. For all the curves in Figs 2–4, the long wavelength limit, $h/l \to 0$ corresponds to the surface mode bifurcation of the substrate and the short wavelength limit, $h/l \to \infty$, corresponds to the surface mode bifurcation of the layer (Hutchinson and Tvergaard, 1980; Dowaikh and Ogden, 1991). For the Mooney–Rivlin material, the values of σ_2/μ in these two limits are equal. For $h/l = 1$, the value of σ_2/μ is very close to the value for the surface mode bifurcation of the layer.

Figure 2 is included for reference and pertains to the case of a perfectly bonded interface. Results for different ratios μ^-/μ^+ are shown. The case $\mu^-/\mu^+ = 1$, not shown, corresponds to the surface instability of a homogeneous half-space for which $\sigma_2/\mu \approx 1.68$. The results in Fig. 2 are consistent with the observation of Papamichos *et al.* (1990) who noted that the stiffer material dominates the development of the instability. If the layer on the half-space is a soft layer then it behaves as a confining medium for the stiff half-space and acts to increase the bifurcation stress above that of the homogeneous half-space. On the other hand, if the material of the layer is stiffer than that of the substrate, then the half-space behaves as a confining medium for the layer. As will be shown in the following, this behavior changes in the presence of interfacial compliance. The bifurcation modes corresponding to the bifurcation stresses in Fig. 2 are stationary wave-like modes which involve both the layer and the substrate. Moreover, when μ^+/μ^- tends to infinity, the

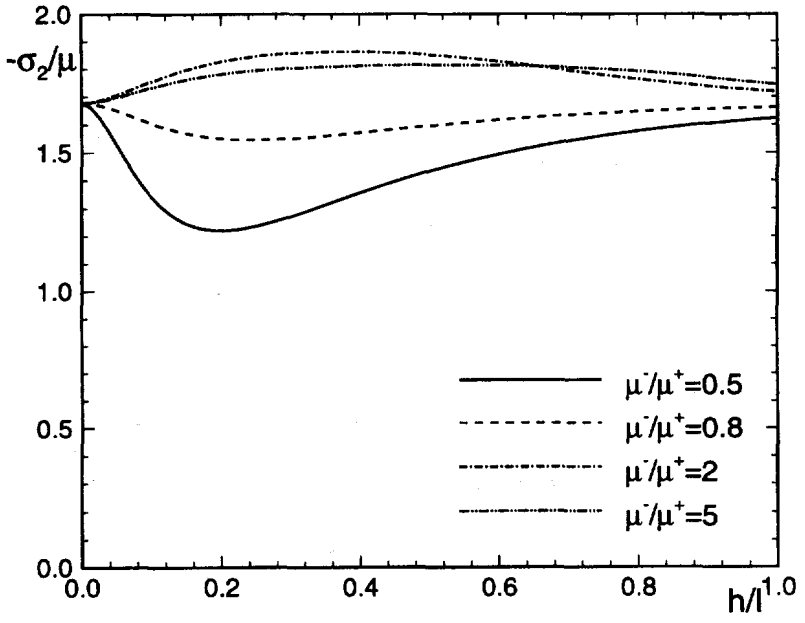

Fig. 2. Bifurcation stress, σ_2, divided by μ, for a layer (+) on a substrate (−) as a function of the layer thickness (h) divided by the wavelength of the bifurcation mode (l). A perfectly bonded interface and different ratios μ^-/μ^+ are considered. The layer and the half-space substrate are both Mooney–Rivlin materials.

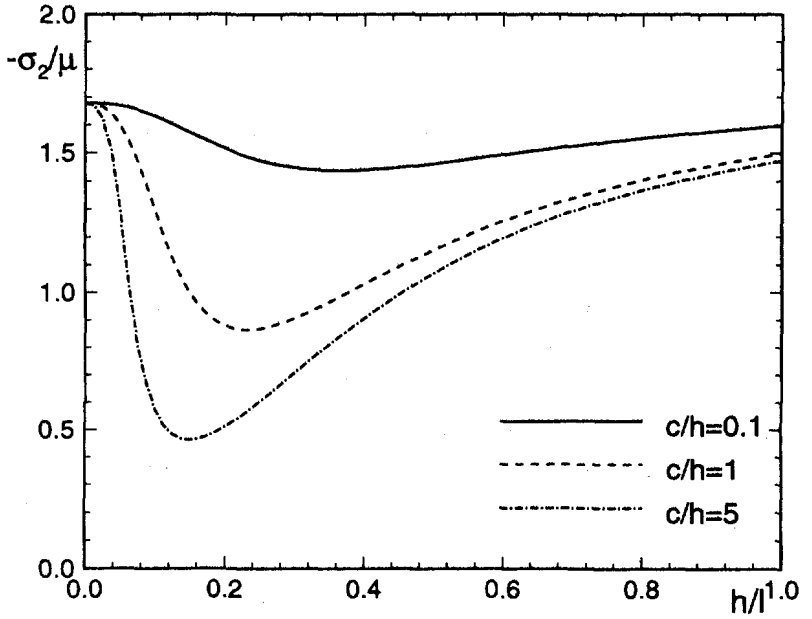

Fig. 3. Bifurcation stress, σ_2, divided by μ, for an elastic half-space with an interface embedded at a depth h as a function of the depth (h) divided by the wavelength of the bifurcation mode (l), for a Mooney–Rivlin material. Various values of interfacial compliance c/h are considered.

solution tends to the bifurcation stress of the layer disconnected from the substrate, i.e., to the case of an isolated layer investigated by Biot (1965), Hill and Hutchinson (1975), and Young (1976). It is also worth noting that the results in Fig. 2 differ from the analogous results of Dorris and Nemat-Nasser (1980) because of their assumption of equal stress in the layer and substrate in the fundamental path.

In Fig. 3, $\mu^-/\mu^+ = 1$, so that the results pertain to an infinitely long, straight interface embedded at depth h in a homogeneous half-space. For small values of c/h, the bifurcation stress differs little from that for a homogeneous half-space for which $\sigma_2/\mu \approx 1.68$. However, for large values of c/h, the minimum bifurcation stress can be reduced by a factor of two or more. Also, for a homogeneous half-space there is no preferred wavelength because there is no characteristic length in the problem. The presence of the compliant interface introduces a characteristic length and a specific wavelength associated with the minimum bifurcation stress. The value of this wavelength increases (h/l decreases) with increasing interface compliance, i.e., increasing values of c/h. In Fig. 3, for a fixed value of c/h, there can be more than one bifurcation mode with the same critical stress. The longer wavelength mode, the smaller value of h/l, corresponds to a plate-like bending mode for the layer while the shorter wavelength mode, the larger value of h/l, corresponds to a surface mode for the layer. The bifurcation mode near the minimum of the curves corresponds to a plate-like bending mode for the layer, which leaves the substrate almost undeformed. This feature is found quite generally when the compliance of the interface is non-zero. The limiting case $c/h \to \infty$ corresponds to zero interface stiffness so that the layer of thickness h acts as an infinitely long (in the x_2-direction) plate, for which the bifurcation stress is zero. Another limiting case is the long wavelength limit, $h/l \to 0$, in which case the critical condition for the surface instability of a half-space is recovered. The strong effect of interfacial compliance on bifurcation is also seen in Keer *et al.* (1982) who considered an array of cracks embedded at depth h and parallel to the free surface.

Figure 4 shows four cases where the stiffness of the layer and the substrate differ. Fig. 4a pertains to a more compliant layer on a stiffer substrate ($\mu^-/\mu^+ = 2$), while Fig. 4b is for a stiffer layer and more compliant substrate ($\mu^-/\mu^+ = 1/2$). In each figure the curve $c/h = 0$ corresponds to the case of a perfectly bonded interface. In Fig. 4a, the substrate is stiffer and the bifurcation stress for a perfectly bonded interface is above that for the isolated substrate. With a non-zero interface compliance, the minimum bifurcation stress

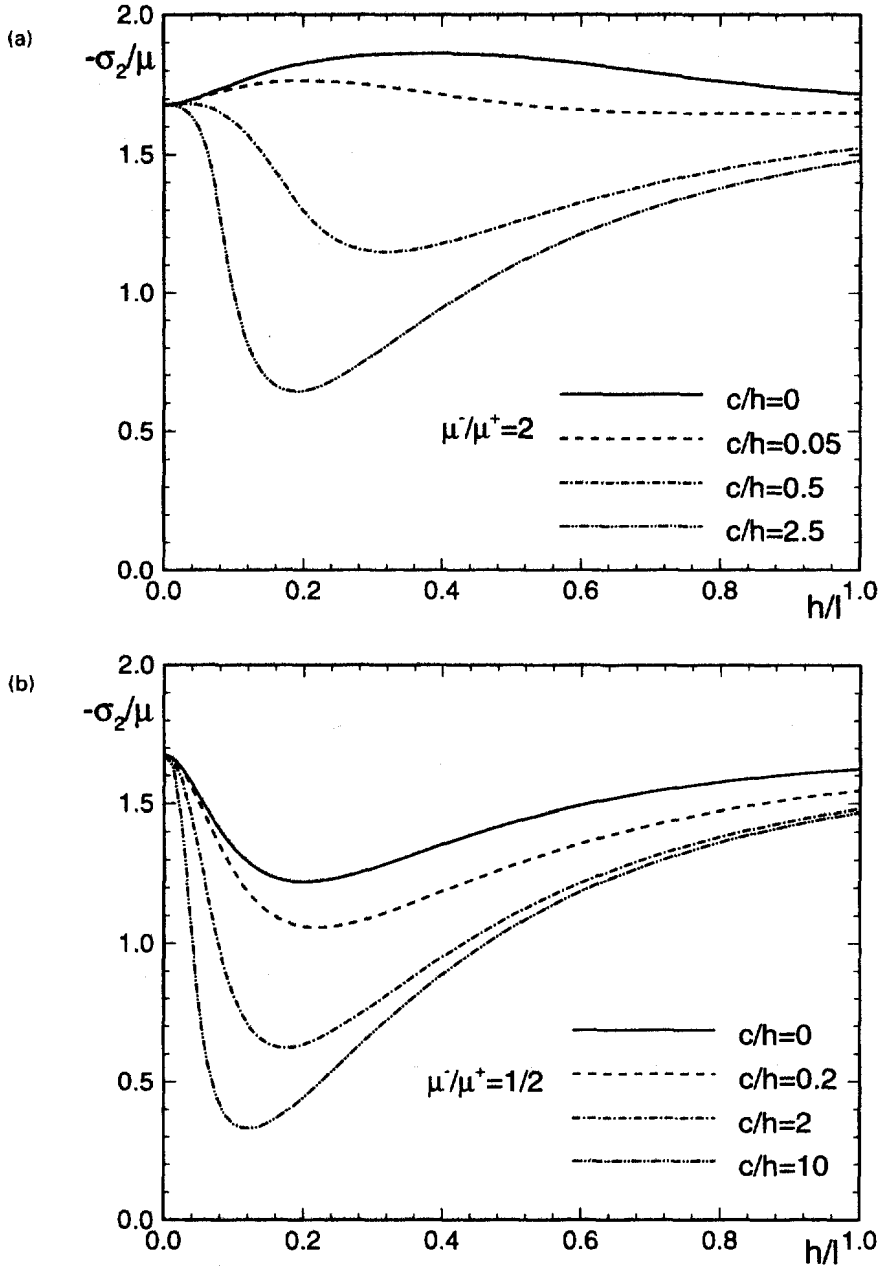

Fig. 4. Bifurcation stress, σ_2, divided by μ, of a layer (+) on an elastic substrate (−) as a function of the layer thickness (h) divided by the wavelength of the bifurcation mode (l). Various values of interfacial compliance c/h are considered. The layer and half-space substrate are both Mooney–Rivlin materials. (a) The layer is weaker than the substrate ($\mu^-/\mu^+ = 2$). (b) The layer is stiffer than the substrate ($\mu^-/\mu^+ = 1/2$).

falls below that for the isolated substrate. In Fig. 4b where the layer is stiffer than the substrate, the shape of the curve of σ_2/μ vs h/l is similar for all values of the interfacial compliance parameter, c/h, with the minimum of the curve decreasing with increasing c/h.

3.1.2. J_2-*deformation theory material.* For this constitutive relation, the layer and substrate are characterized by the two material parameters N^+, K^+, and N^-, K^-, respectively, where the parameter K has the dimensions of stress and is defined by

$$K = \frac{\sigma_0}{\varepsilon_0^N}\left(\frac{2}{\sqrt{3}}\right)^{N+1}. \tag{37}$$

It is convenient to characterize the current state by the logarithmic strain $\varepsilon = \ln \lambda$. From (14), the current stress state is specified by $\sigma_1 = 0$ and $\sigma_2 = -K\varepsilon^N$. The determinant (29), is now considered a function of ε and the bifurcation condition is expressed as a critical value of the logarithmic strain, ε, instead of as a critical stress value.

The logarithmic strain at bifurcation is plotted against h/l in Fig. 5 for different values of the parameter c/h defined in (33). The results in Fig. 5a are for $K^-/K^+ = 2$, $N^+ = 0.1$, $N^- = 0.4$, while those in Fig. 5b are for $K^-/K^+ = 1/2$, $N^+ = 0.1$, $N^- = 0.4$, and those in Fig. 5c for $K^-/K^+ = 2$, $N^+ = 0.4$, $N^- = 0.1$. For the case in Fig. 5a the magnitude of the stress in the substrate exceeds that in the layer when $\varepsilon > 0.099$. On the other hand, the magnitude of the stress in the layer exceeds that in the substrate over the entire range in Fig. 5b. In Fig. 5c, the properties of the layer and substrate are reversed from those in Fig.

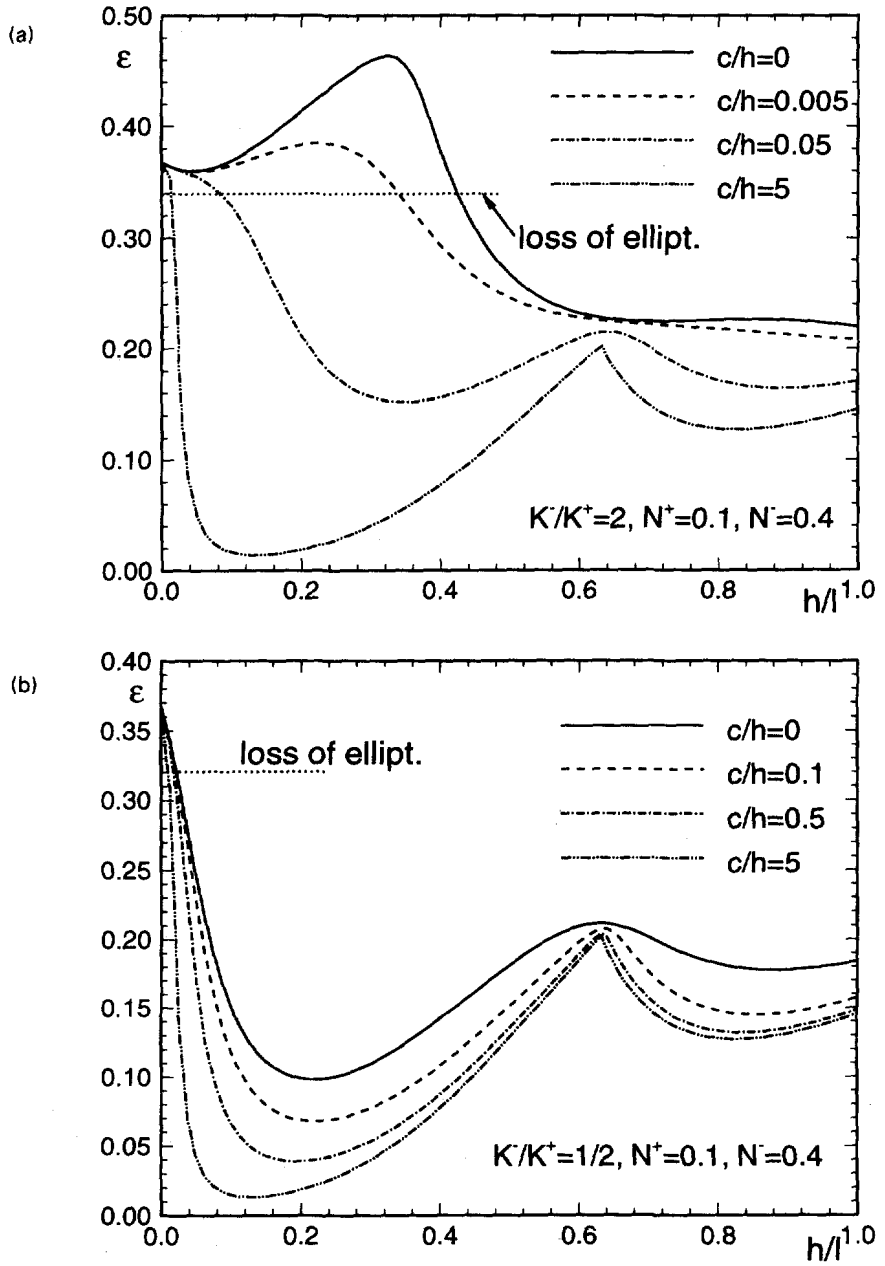

Fig. 5. Logarithmic strain at bifurcation, ε, for a layer (+) on an elastic substrate (−) as a function of the layer thickness (h) divided by the wavelength of the bifurcation mode (l). Various values of interfacial stiffness c/h are considered. The layer and the half-space substrate are both J_2-deformation theory materials. (a) $K^-/K^+ = 2$, $N^+ = 0.1$, $N^- = 0.4$. (b) $K^-/K^+ = 1/2$, $N^+ = 0.1$, $N^- = 0.4$. (c) $K^-/K^+ = 2$, $N^+ = 0.4$, $N^- = 0.1$.

(c)

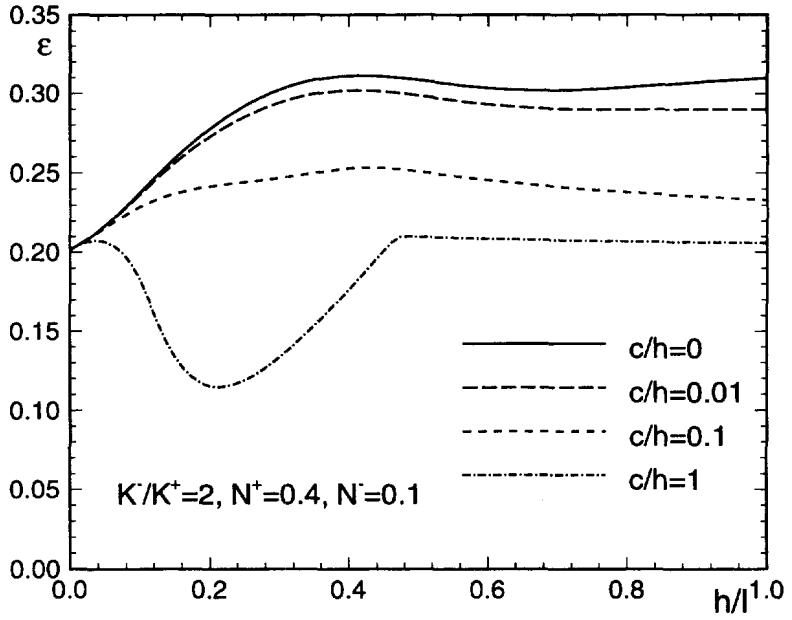

Fig. 5—*Continued*

5b so that here the magnitude of the stress in the substrate exceeds that in the layer over the range shown.

For the J_2-deformation theory solid, loss of ellipticity may occur before bifurcation into the diffuse mode. This is indeed the case for the initial portions of the graphs in Figs 5a and 5b, where loss of ellipticity occurs in the layer; with $N^+ = 0.1$ this occurs at $\varepsilon \approx 0.32$. The portion of the curves falling above this value (denoted in the graphs by a horizontal dotted line) corresponds to circumstances where strain localization terminates the homogeneous response along the fundamental path and diffuse bifurcation modes become available subsequently. The stiffer the interface, the larger the regime in which homogeneous deformation is terminated by strain localization in the layer. In Fig. 5c, bifurcation always occurs in the elliptic range.

In the long wavelength limit, $h/l \to 0$, the critical condition for a surface instability of the substrate is approached, for all curves in Fig. 5. In contrast to the Mooney–Rivlin material, the short wavelength limit may correspond to the surface mode being the one at the layer–half-space interface. This is the case in Fig. 5c, where, for a perfectly bonded interface, the solution tends to the interfacial bifurcation mode and strain in the short wavelength limit $h/l \to \infty$. This is due to the fact that the critical strain for the interfacial mode is less than that corresponding to a free surface instability of the layer. For finite stiffness of the interface, the solution tends once more to that for an interfacial instability and, slowly, to the surface bifurcation strain of the half-space. This agrees with results for interfacial bifurcation, in the presence of an interface of the type (6): the surface bifurcation strain of the half-space more prone to instability is approached in the short wavelength limit.

For a better understanding of Fig. 5c, follow the curve relative to $c/h = 1$, for h/l increasing. Initially the bifurcation strain corresponds to the surface instability mode for the substrate. Then, the bonding to the layer leads to a very small increase in this bifurcation strain. The critical mode soon evolves into a plate-like buckling mode for the layer (corresponding to the minimum of the curve). This mode remains close to the isolated layer solution, until a flat portion of the curve, where an interfacial bifurcation mode becomes available. This interfacial bifurcation mode slowly tends to the surface bifurcation mode of the substrate, for h/l increasing.

3.2. *Layer on an undeforming substrate*

In this section the special case of a layer connected through an interface of the type (6) to an undeforming substrate is considered. The substrate, however, is supposed to

follow the deformation of the layer in the fundamental path, until bifurcation occurs. Since the only material properties that enter are those of the layer, the superscript + associated with layer quantities is dropped. The fundamental solution is one of compression parallel to the layer so that $\sigma_1 = 0$ and $\sigma_2 < 0$. Therefore, the layer is subject to traction free conditions on one side, at $x_1 = 0$, whereas it is subject to the interface conditions (6), with $v_k^- = 0$, on the other side, at $x_1 = h$. The bifurcation condition becomes

$$\det(\mathbf{N}) = 0, \tag{38}$$

where $\mathbf{N}$ is the 4×4 coefficient matrix of the system of equations

$$\begin{bmatrix} N_{11} & N_{12} & N_{13} & N_{14} \\ N_{21} & N_{22} & N_{23} & N_{24} \\ N_{31} & N_{32} & N_{33} & N_{34} \\ N_{41} & N_{42} & N_{43} & N_{44} \end{bmatrix} \begin{bmatrix} b_1 \\ b_2 \\ b_3 \\ b_4 \end{bmatrix} = \begin{bmatrix} 0 \\ 0 \\ 0 \\ 0 \end{bmatrix}. \tag{39}$$

The expressions for the components of $\mathbf{N}$ are given in the Appendix assuming that $S_{12} = S_{21} = 0$.

The bifurcation condition (38) involves the ratio μ/μ_* and depends on the length parameters kh and c, where, as in the previous results, the assumption $\delta_n/C_n = \delta_t/C_t$ is made so that there is a single interface characteristic length given by (33). In the limit $\mathbf{S} \to 0$, the results for a free layer are recovered.

In Fig. 6 bifurcation results are presented as a function of μ/μ_*, without assuming any specific dependence of μ or μ_* on stress or deformation. Results for $\mu/\mu_* = 1/3$, 1 and 3 are shown in Figs 6a, 6b and 6c, respectively. In each figure, the critical compressive stress, normalized by the modulus μ_* is plotted against h/l, the ratio of layer thickness to bifurcation mode wave length. In each case results for various values of the ratio of layer thickness, h, to interface characteristic length, c, are plotted; $h/c = 0$ corresponds to a free layer, $C_n = C_t = 0$, and increasing values of this ratio correspond to increasing interface stiffness. For fixed values of the interface stiffness parameters C_n and C_t, increasing h/c corresponds to increasing layer thickness.

For $h/c = 0$, the minimum bifurcation stress is associated with a column buckling mode for a column of zero aspect ratio and is, therefore, zero. With increasing interface stiffness (or increasing layer thickness) the minimum bifurcation stress increases and the wavelength of the corresponding bifurcation mode decreases. For a very stiff interface, or a very thick layer, $h/c \to \infty$, the minimum bifurcation stress tends to the critical stress for a surface instability of the layer. For $\mu/\mu_* = 1/3$, 1 and 3, the critical values of $-\sigma_2/\mu_*$ for a surface instability are 0.64, 1.68 and 3.73, respectively. For long wavelengths, $h/l \to 0$ the curves for $h/c > 0$ are terminated at the value of σ_2/μ_* for which ellipticity is lost in the layer. These values are $\sigma_2/\mu_* = -2/3$ for $\mu/\mu_* = 1/3$ in Fig. 6a, $\sigma_2/\mu_* = -2$ for $\mu/\mu_* = 1$ in Fig. 6b and $\sigma_2/\mu_* = -4\sqrt{2}$ for $\mu/\mu_* = 3$ in Fig. 6c.

Results for J_2-deformation theory materials are shown in Fig. 7, with $N = 0.1$ in Fig. 7a, and with $N = 0.4$ in Fig. 7b. Here, the strain for bifurcation is plotted against h/l. In Fig. 7a, where $N = 0.1$, loss of ellipticity occurs at $\varepsilon \approx 0.32$ and the strain at which a surface instability occurs is $\varepsilon \approx 0.20$. For $N = 0.4$ these values are $\varepsilon \approx 0.68$ and $\varepsilon \approx 0.37$, respectively. In Fig. 7a, for $h/c > 0$, there are two local minima; the one corresponding to the longer wavelength, i.e., the smaller value of h/l, is the absolute minimum for smaller values of h/c, but the larger value of h/l is the absolute minimum for a stiffer interface or a thicker layer, i.e., a larger value of h/c. On the other hand, for $N = 0.4$, the longer wavelength mode, i.e., the smaller value of h/l, is the absolute minimum in all cases shown. In both Figs 6 and 7 the strong effect of a compliant interface in precipitating bifurcation can be seen.

In Fig. 8, we consider the special case $S_{22} = 0$, with $S_{11} \neq 0$. This case corresponds to a layer on "continuously distributed transverse springs", analogous to a Winkler foundation. The predictions based on (38) and (39) are compared with results obtained from approximate Kirchhoff plate theory. Approximations of this type have been used in previous investigations of the stability of layered solids, e.g., Shield *et al.* (1994). In order to obtain this approximation under the present constitutive assumptions, consider a layer of current thickness h in the x_1–x_2-plane, where x_2 has the direction of the bond line and $x_1 \in [-h/2, h/2]$. Before bifurcation, the layer is subject to a state of compression parallel to x_2, so that the only non-zero component of Cauchy stress is $\sigma_2 < 0$. In these circumstances, Biot (1965, Sect. 2) has shown that equilibrium requires

$$M_{,22} + m_{,2} + q + h\sigma_2 v_{1,22} = 0, \tag{40}$$

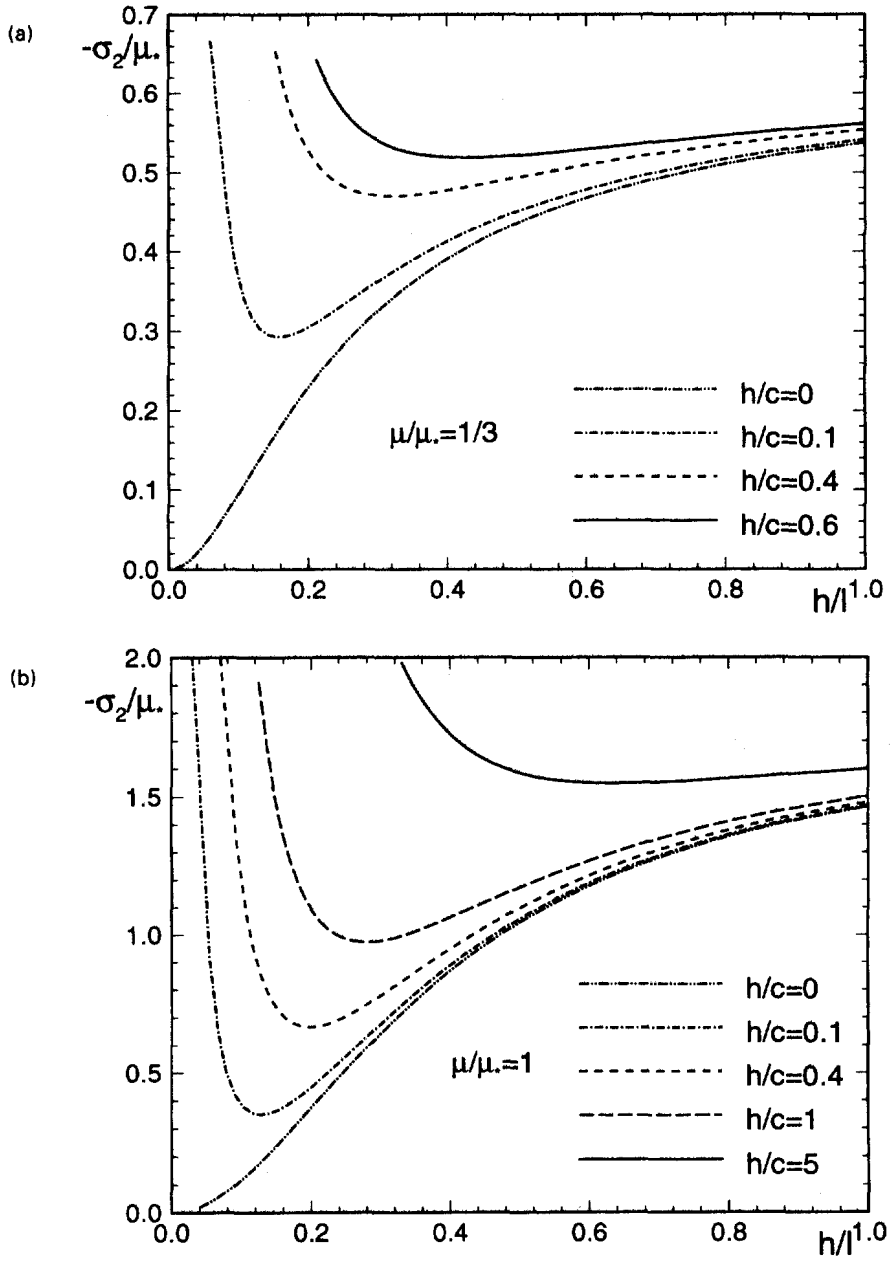

Fig. 6. Bifurcation stress, σ_2, divided by μ_*, for a layer on an undeforming substrate, as a function of the layer thickness (h) divided by the wavelength of the bifurcation mode (l). Various values of interfacial stiffness h/c are considered. (a) $\mu/\mu_* = 1/3$. (b) $\mu/\mu_* = 1$. (c) $\mu/\mu_* = 3$.

(c)

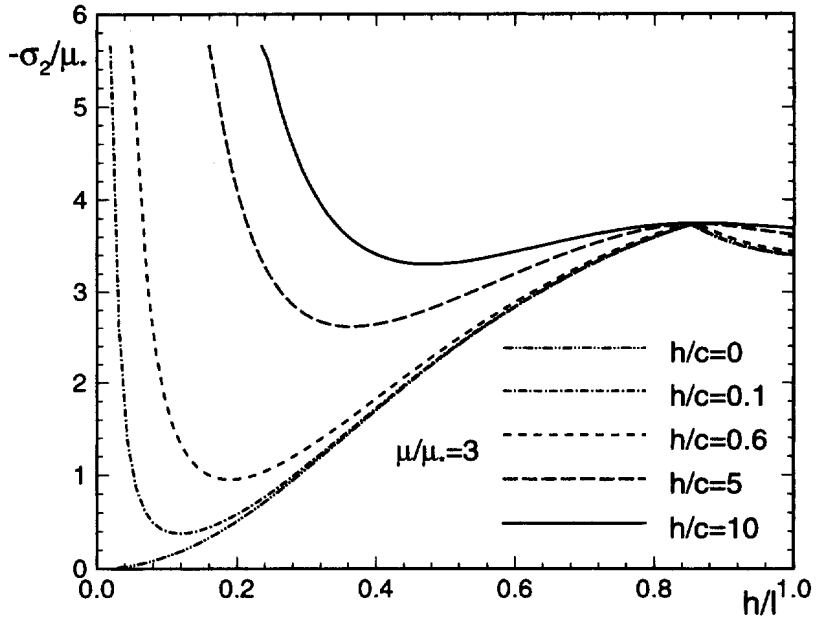

Fig. 6—*Continued*

where

$$M = \int_{-h/2}^{+h/2} x_1 \dot{t}_{22}\, dx_1, \quad m = \dot{t}_{12} x_1|_{x_1=h/2} - \dot{t}_{12} x_1|_{x_1=-h/2},$$

$$q = \dot{t}_{11}|_{x_1=h/2} - \dot{t}_{11}|_{x_1=-h/2}, \quad \bar{v}_1 = \frac{1}{h}\int_{-h/2}^{+h/2} v_1\, dx_1. \tag{41}$$

Because the tangential stiffness of the interface vanishes, i.e., $S_{22} = 0$, $m = 0$, and $q = -S_{11}\bar{v}_1$ and therefore (40) becomes

$$M_{,22} - S_{11}\bar{v}_1 + h\sigma_2 \bar{v}_{1,22} = 0. \tag{42}$$

The plate theory deformation assumption is

$$\bar{v}_1 = w(x_2) \quad v_2 = u_0(x_2) - x_1 w_{,2}, \tag{43}$$

so that $d_{12} = 0$. Also, each layer of the plate is assumed to be in a state of plane stress so that

$$\dot{t}_{11} = \dot{\sigma}_{11} = 0, \tag{44}$$

and, therefore, from (2), (10) and incompressibility, (3), $\dot{p} = 2\mu_* v_{2,2}$ so that

$$\dot{t}_{22} = (4\mu_* - \sigma_2) v_{2,2}. \tag{45}$$

Using (43) in (44), M can be calculated and substituting into (42) gives

$$D_* \frac{d^4 w}{dx_2^4} - \sigma_2 h \frac{d^2 w}{dx_2^2} + S_{11} w = 0, \tag{46}$$

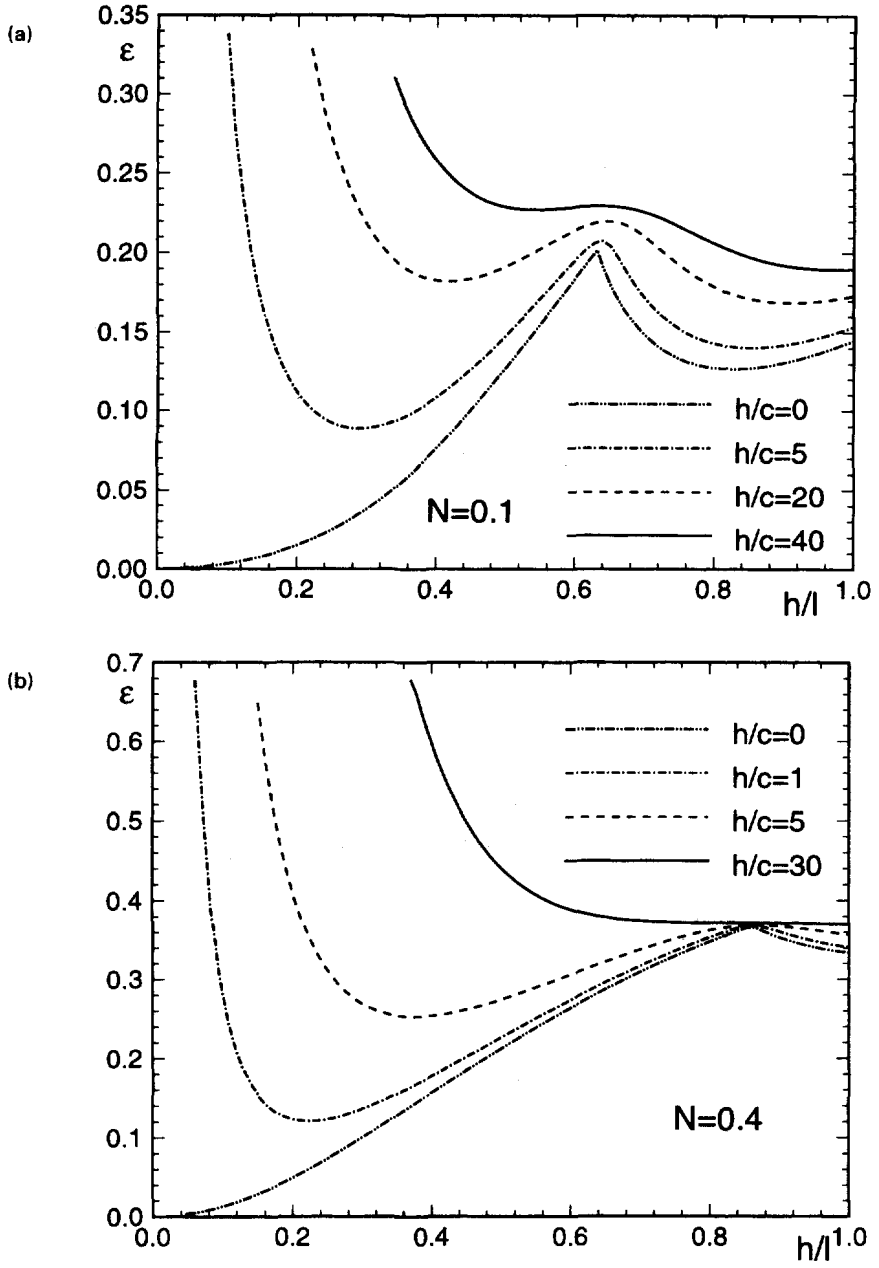

Fig. 7. Logarithmic strain at bifurcation, ε, for a layer on an undeforming substrate as a function of the layer thickness (h) divided by the wavelength of the bifurcation mode (l) for J_2-deformation theory materials. Various values of interfacial stiffness h/c are considered. (a) $N = 0.1$. (b) $N = 0.4$.

where

$$D_* = \frac{h^3}{12}(4\mu_* - \sigma_2). \tag{47}$$

Note that (42) is exact (as remarked by Biot, 1965), whereas (46) is approximate, because of both the assumptions of plane stress and the plate theory deformation mode (43).

For an infinite (in the x_2-direction) plate, write

$$w(x_2) = A\sin(kx_2) \tag{48}$$

where $k = n\pi/l$ is the bifurcation mode wavelength.

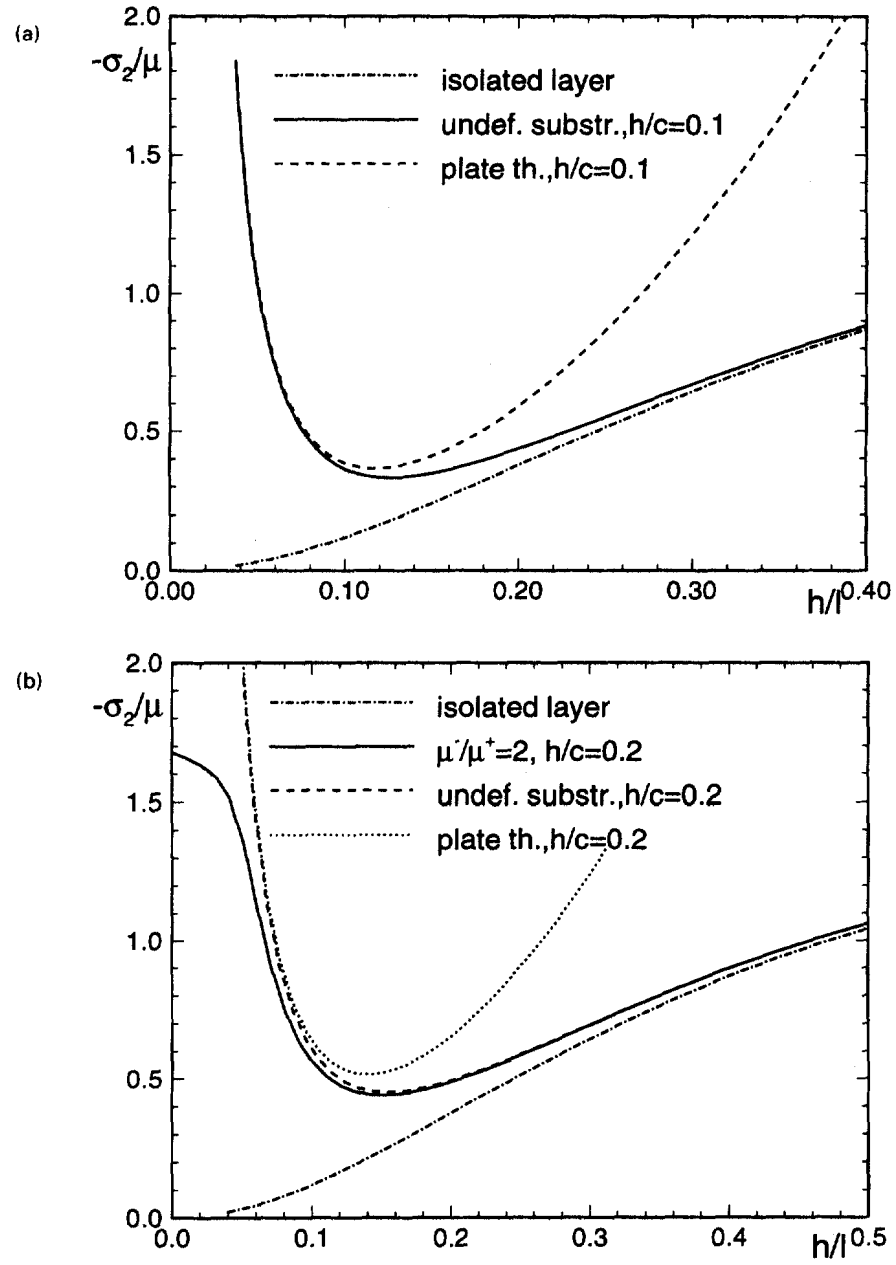

Fig. 8. Bifurcation stress, divided by μ for a layer on an undeforming substrate (with $S_{22} = 0$) and for an isolated layer ($S_{11} = S_{22} = 0$), for a Mooney–Rivlin material, compared with the plate theory approximation (50). In (b) results for a layer on an elastic half-space with $\mu^-/\mu^+ = 2$ are also shown.

Solving for $\sigma_2 h$ results in

$$-\sigma_2 h = D^* k^2 + S_{11}\frac{1}{k^2}. \tag{49}$$

Assuming that $4\mu_* \gg |\sigma_2|$ and using (33), (49) can be written as

$$-\frac{\sigma_2}{\mu_*} = \frac{1}{3}(kh)^2 + \frac{h}{c}\frac{1}{(kh)^2}. \tag{50}$$

It is expected that (50) will give a good approximation to the layer on elastic foundation

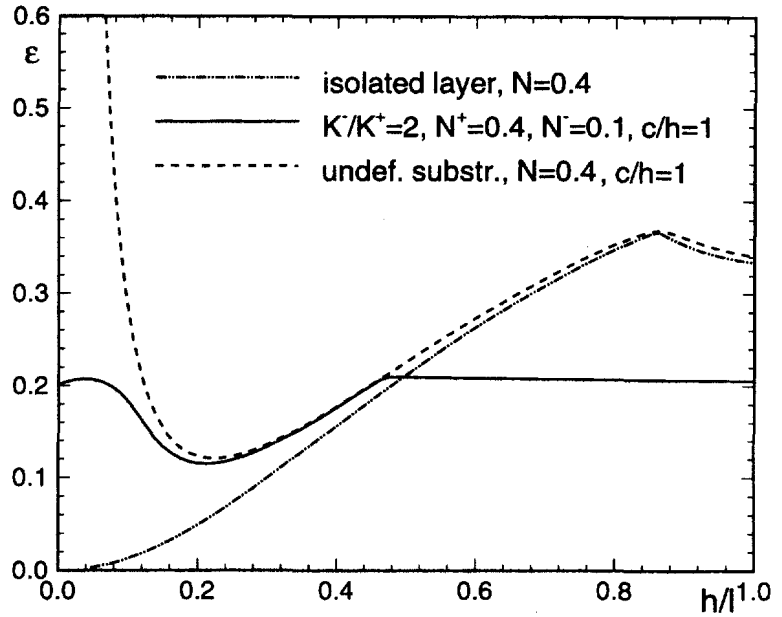

Fig. 9. Logarithmic strain at bifurcation, ε, for a layer on an undeforming substrate for a J_2-deformation theory material and for an isolated layer with $N = 0.4$, compared with a layer on an elastic substrate with $K^-/K^+ = 2$, $N^+ = 0.4$, $N^- = 0.1$.

problem when h/l and c/h are sufficiently small. Figure 8 shows a comparison of the solution based on (38) and (39) with the approximation (50) for a Mooney–Rivlin material. Also included are results for an isolated layer and, in Fig. 8b, for a layer on an elastic half-space, in order to illustrate the approximation involved in idealizing the half-space as undeforming. The results for a layer on an elastic half-space differ from those in Section 3.1 in that in Fig. 8b $S_{22} = 0$. In Fig. 8a $h/c = 0.1$, while in Fig. 8b $\mu^-/\mu^+ = 2$ and $h/c = 0.2$. Note that for $-\sigma_2/\mu$ higher than about 0.3, the approximations made in leading to (50) (including $4\mu \gg |\sigma_2|$) are not necessarily accurate. Nevertheless, over a fairly wide range the approximation is reasonably good. Other results for $h/c = 0.01$ and smaller (not shown here) indicate that (50) gives a good approximation of the minimum value of the bifurcation stress. Similar calculations were carried out using J_2-deformation theory with $N = 0.1$ (also not shown here) and, as in Fig. 8, the results for a layer on an elastic foundation are qualitatively similar to those for a layer on elastic-half space, except close to the long wavelength limit $h/l = 0$. This is not the case for the J_2-deformation theory solid with $N = 0.4$ in Fig. 9 because of the occurrence of an interfacial bifurcation between the layer and the half-space that is not possible for the layer on an elastic foundation.

4. CONCLUDING REMARKS

The bifurcation of a layer bonded to a substrate has been analyzed allowing for interfacial compliance. The substrate is idealized as a half-space and the compliant interface is described by an incrementally linear constitutive law between the nominal traction rate and the velocity jump across the interface. Plane strain conditions have been assumed and the layer and substrate materials were taken to be hyperelastic, incompressible and orthotropic. Specific examples have been given with the layer and substrate materials modeled as Mooney–Rivlin and J_2-deformation theory materials. The special case of a layer on an undeforming substrate has also been considered.

A variety of bifurcation modes are possible depending on the layer thickness, on the constitutive parameters of the layer and the substrate, and on the interface compliance. These modes include shear band modes for the layer and the substrate, and a surface instability mode for the layer that are unaffected by the compliance of the interface. Diffuse bifurcation modes that involve deformation of both the layer and the substrate are affected

by the compliance of the interface. For large interfacial compliance, there is also a plate-like bending mode for the layer that leaves the substrate almost undeformed.

Because the constitutive relation for the interface is a relation between the nominal traction rate and the velocity jump across the interface, a characteristic length is introduced. In the numerical results presented here we assume that the interface compliance matrix has only one non-vanishing component (or two equal components). The ratio of the characteristic interface length, c defined by (33) to the layer thickness h then characterizes the role of the interface compliance. For a perfectly bonded interface $c/h = 0$ $(h/c \to \infty)$, while a free surface between the layer and substrate corresponds to $c/h \to \infty$ $(h/c = 0)$.

From (33) the ratio c/h can be written as (δ_n/h) (μ_*^+/C_n). The first term is the ratio of an interface characteristic length to the layer thickness which is expected to be small, say of the order of 10^{-3} or smaller. For a well bonded interface, the second term would be of the order of unity. Hence, c/h would be very small and the interface compliance would play a negligible role on the bifurcation behavior. However, when the bond between the layer and substrate is weak, the interface stiffness C_n is small and the ratio (μ_*^+/C_n) can be large. In such a situation c/h can be large enough to substantially affect bifurcation even though (δ_n/h) is small. It is also worth noting that because the compliance of the interface is expected to vary with the normal traction across it, the onset of bifurcation in the circumstances analyzed would depend on whether or not the layer and substrate were subject to an all around hydrostatic tension or compression, even though the materials considered here are incompressible.

Quite generally, in the cases considered here, the lowest bifurcation stress corresponds to the plate like bending mode for the layer with a wavelength of from 5 to 20 times the layer thickness. This mode can be critical even when the layer and interface are bonded; complete debonding is not required. This mode is not available for a perfectly bonded layer so the reduction in critical stress due to interface compliance is substantial. In some cases, for example in Figs 6c and 7a, there is also a shorter wavelength regime where the bifurcation stress is reduced because of the compliance of the interface. However, for the problem considered in which the length parallel to the interface is infinite, the longer wavelength plate-like mode gives a lower bifurcation stress.

Suppose a layer bonded to a substrate is considered where the bond is weak along a segment of the interface. If this weakly bonded segment is very long compared to the layer thickness, the result for an infinitely long layer is expected to apply and the plate-like mode would be critical. Bifurcation into the plate-like mode can occur with very small pre-bifurcation strains. On the other hand, if the length of the weakly bonded segment is of the order of the layer thickness or less, the bifurcation mode involves coupled deformations of the layer, and bifurcation only occurs after large strains (or large values of $|\sigma_2/\mu|$). Then, depending on material properties, there may, e.g. Fig. 5a, or may not, e.g. Fig. 5b, be a significant effect of interfacial compliance on precipitating bifurcation. Accordingly, in a specific circumstance, the bifurcation mode observed would be expected to depend on the extent of the region of weak bonding as well as on the material and interface properties.

It is worth noting that although attention has been focused on a layer on a half-space substrate the general formulation, through a change in boundary conditions, can readily be extended to consider more general layered solids.

Acknowledgements—D.B. gratefully acknowledges the financial support of Italian M.U.R.S.T. 40%—1995 and thanks the Brown Exchange Program for having supported his visit to Brown University. M.O. and A.N. are grateful for support from the Materials Research Group on Micro- and Nano-Mechanics of Failure-Resistant Materials, funded at Brown University under NSF Grant DMR-9002994.

REFERENCES

Benallal, A., Billardon, R. and Geymonat, G. (1993) Bifurcation and localization in rate-independent materials. Some general considerations. In *Bifurcation and Stability of Dissipative Systems*, ed. Q. S. Nguyen. Springer-Verlag, Vienna–New York.

Biot, M. A. (1965) *Mechanics of Incremental Deformation*. Wiley, New York.

Christofferson, J. and Hutchinson, J. W. (1979) A class of phenomenological corner theories of plasticity. *Journal of the Mechanics and Physics of Solids* **27**, 465–487.

Dorris, J. F. and Nemat-Nasser, S. (1980) Instability of a layer on a half space. *Journal of Applied Mechanics* **47,** 304–312.
Dowaikh, M. A. and Ogden, R. W. (1990) On surface waves and deformations in a pre-stressed incompressible elastic solid. *IMA Journal of Applied Mathematics* **44,** 261–284.
Dowaikh, M. A. and Ogden, R. W. (1991) Interfacial waves and deformations in a pre-stressed elastic media. *Proceedings of the Royal Society of London A* **443,** 313–328.
Hill, R. (1958) A general theory of uniqueness and stability in elastic–plastic solids. *Journal of the Mechanics and Physics of Solids* **6,** 236–249.
Hill, R. and Hutchinson, J. W. (1975) Bifurcation phenomena in the plane tension test. *Journal of the Mechanics and Physics of Solids* **23,** 239–264.
Hutchinson, J. W. and Neale, K. W. (1979) Finite strain J_2-deformation theory. In *Proc. IUTAM Symp. on Finite Elasticity*, eds D. E. Carlson and R. T. Shield. Martinus Nijhoff, The Hague–Boston–London, pp. 237–247.
Hutchinson, J. W. and Tvergaard, V. (1980). Surface instabilities on statically strained plastic solids. *International Journal of Mechanical Sciences* **22,** 339–354.
Hutchinson, J. W. and Tvergaard, V. (1981). Shear band formation in plane strain. *International Journal of Solids and Structures* **17,** 451–470.
Keer, L. M., Nemat-Nasser, S. and Oranratnachai, A. (1982) Surface instability and splitting in compressed brittle elastic solids containing crack arrays. *Journal of Applied Mechanics* **49,** 761–767.
Ogden, R. W. and Sotiropoulus, D. A. (1995) On interfacial waves in pre-stressed layered incompressible elastic solid. *Proceedings of the Royal Society of London A* **450,** 319–341.
Özturk, T., Poole, W. J. and Embury, J. D. (1991) The deformation of Cu–W laminates. *Materials Science Engineering* **A148,** 175–178.
Papamichos, E., Vardoulakis, I. and Mühlaus, H.-B. (1990) Buckling of layered elastic media: a Cosserat-continuum approach and its validation. *International Journal of Numerical and Analytical Methods in Geomechanics* **14,** 473–498.
Shield, T. W., Kim, K. S. and Shield, R. T. (1994) The buckling of an elastic layer bonded to an elastic substrate in plane strain. *Journal of Applied Mechanics* **61,** 231–235.
Suo, Z., Needleman, A. and Ortiz, M. (1992) Stability of solids with interfaces. *Journal of the Mechanics and Physics of Solids* **40,** 613–640.
Steif, P. F. (1986a) Bimaterial interface instabilities in plastic solids. *International Journal of Solids and Structures* **22,** 195–207.
Steif, P. F. (1986b) Periodic necking instabilities in layered plastic solids. *International Journal of Solids and Structures* **22,** 1571–1578.
Steif, P. F. (1987) An exact two dimensional approach to fiber micro-buckling. *International Journal of Solids and Structures* **23,** 1235–1246.
Steif, P. F. (1990) Interfacial instabilities in an unbounded layered solid. *International Journal of Solids and Structures* **26,** 915–925.
Steigmann, D. J. and Ogden, R. W. (1996) Plane deformations of elastic solids with intrinsic boundary elasticity. Submitted.
Triantafyllidis, N. and Lehner, F. K. (1993) Interfacial instability of density-stratified two-layer systems under initial stress. *Journal of the Mechanics and Physics of Solids* **41,** 117–142.
Triantafyllidis, N. and Leroy, Y. M. (1994) Stability of a frictional material layer resting on a viscous half-space. *Journal of the Mechanics and Physics of Solids* **42,** 51–110.
Young, N. B. J. (1976) Bifurcation phenomena in the plane compression test. *Journal of the Mechanics and Physics of Solids* **24,** 77–91.

APPENDIX

The components of **M** in (30) are:

$$M_{11} = A^+\tau_1^+, \quad M_{12} = -M_{11} \tag{51}$$

$$M_{13} = D^+\tau_3^+, \quad M_{14} = -M_{13} \tag{52}$$

$$M_{15} = M_{16} = 0 \tag{53}$$

$$M_{21} = B^+ + C^+\left(\frac{\tau_1^+}{k}\right)^2, \quad M_{22} = M_{21} \tag{54}$$

$$M_{23} = B^+ + C^+\left(\frac{\tau_3^+}{k}\right)^2, \quad M_{24} = M_{23} \tag{55}$$

$$M_{25} = M_{26} = 0 \tag{56}$$

$$M_{31} = A^+\tau_1^+\exp(\tau_1^+ h), \quad M_{32} = -A^+\tau_1^+\exp(-\tau_1^+ h) \tag{57}$$

$$M_{33} = D^+\tau_3^+\exp(\tau_3^+ h), \quad M_{34} = -D^+\tau_3^+\exp(-\tau_3^+ h) \tag{58}$$

$$M_{35} = A^-\tau_1^-, \quad M_{36}D^-\tau_3^- \tag{59}$$

$$M_{41} = M_{21}\exp(\tau_1^+ h), \quad M_{42} = M_{21}\exp(-\tau_1^+ h) \tag{60}$$

$$M_{43} = M_{23}\exp(\tau_3^+ h), \quad M_{44} = M_{23}\exp(-\tau_3^+ h) \tag{61}$$

$$M_{45} = -B^- - C^-\left(\frac{\tau_1^-}{k}\right)^2, \quad M_{46} = -B^- - C^-\left(\frac{\tau_3^-}{k}\right)^2 \tag{62}$$

$$M_{51} = \exp(\tau_1^+ h), \quad M_{52} = \exp(-\tau_1^+ h) \tag{63}$$

$$M_{53} = \exp(\tau_3^+ h), \quad M_{54} = \exp(-\tau_3^+ h) \tag{64}$$

$$M_{55} = -\frac{A^-\tau_1^-}{S_{11}} - 1, \quad M_{56} = -\frac{D^-\tau_3^-}{S_{11}} - 1 \tag{65}$$

$$M_{61} = \frac{\tau_1^+}{k}\exp(\tau_1^+ h), \quad M_{62} = -\frac{\tau_1^+}{k}\exp(-\tau_1^+ h) \tag{66}$$

$$M_{63} = \frac{\tau_3^+}{k}\exp(\tau_3^+ h), \quad M_{64} = -\frac{\tau_3^+}{k}\exp(-\tau_3^+ h) \tag{67}$$

$$M_{65} = \left[B^- + C^-\left(\frac{\tau_1^-}{k}\right)^2\right]\frac{k}{S_{22}} + \frac{\tau_1^-}{k}, \quad M_{66} = \left[B^- + C^-\left(\frac{\tau_3^-}{k}\right)^2\right]\frac{k}{S_{22}} + \frac{\tau_3^-}{k} \tag{68}$$

where

$$A = \left(2\mu_* - p + \frac{\Lambda}{2}\right), \quad B = \mu - p, \quad C = \mu + \frac{\sigma}{2}, \quad D = \left(2\mu_* - p - \frac{\Lambda}{2}\right). \tag{69}$$

The components of **N** in (39) are:

$$N_{11} = A\tau_1, \quad N_{12} = -N_{11} \tag{70}$$

$$N_{13} = D\tau_3, \quad N_{14} = -N_{13} \tag{71}$$

$$N_{21} = B + C\left(\frac{\tau_1}{k}\right)^2, \quad N_{22} = N_{21} \tag{72}$$

$$N_{23} = B + C\left(\frac{\tau_3}{k}\right)^2, \quad N_{24} = N_{23} \tag{73}$$

$$N_{31} = \left(A\frac{\tau_1}{k} + \frac{S_{11}}{k}\right)\exp(\tau_1 h), \quad N_{32} = \left(-A\frac{\tau_1}{k} + \frac{S_{11}}{k}\right)\exp(-\tau_1 h), \tag{74}$$

$$N_{33} = \left(D\frac{\tau_3}{k} + \frac{S_{11}}{k}\right)\exp(\tau_3 h), \quad N_{34} = \left(-D\frac{\tau_3}{k} + \frac{S_{11}}{k}\right)\exp(-\tau_3 h), \tag{75}$$

$$N_{41} = \left[B + C\left(\frac{\tau_1}{k}\right)^2 + \frac{S_{22}\tau_1}{k^2}\right]\exp(\tau_1 h), \quad N_{42} = \left[B + C\left(\frac{\tau_1}{k}\right)^2 - \frac{S_{22}\tau_1}{k^2}\right]\exp(-\tau_1 h), \tag{76}$$

$$N_{43} = \left[B + C\left(\frac{\tau_3}{k}\right)^2 + \frac{S_{22}\tau_3}{k^2}\right]\exp(\tau_3 h), \quad N_{44} = \left[B + C\left(\frac{\tau_3}{k}\right)^2 - \frac{S_{22}\tau_3}{k^2}\right]\exp(-\tau_3 h), \tag{77}$$

where A, B, C and D are still defined by (69).